Design and Fracture Analysis of Horizontal Axis Wind Turbine Blade

Santhosh kumar V[1], Dr.M.Sekar[2]
[1]Dept of Mechanical engineering
[2]Associate professor, Dept of Mechanical engineering
[1, 2] Government College of Technology Coimbatore

Abstract- *Horizontal axis wind turbines (HAWT) constitute the most common type of wind turbine in use today. The blades of the wind turbines are more prone to fracture. Broken blades are the important factor of this project. Rotor blades up to 1.5 tones and can travel at over 180 mph. They can cause massive problems if these blades were to brake. Failure of blades leads to interrupted supply of energy and it should be eliminated. Even a single blade gets fractured in a 3-rotor blade arrangement; all the three blades need replacement to ensure dynamic balancing condition, which involves huge amount of money. The main intention of this project is to eradicate the catastrophic failure of the wind turbine rotor blade. The blade to be analyzed is made up of Fiber Reinforced Polyester material. Blade line load has to be carried out as per DS 472 standard. The model has to be created in SOLID WORKS. Fracture Mechanics approach of crack analysis will be performed. Stress Intensity Factor on each crack propagation, under various wind loads using ANSYS has to be done. Analytical determination of Stress Intensity Factor has been calculated for each crack length under various load conditions using J integral.*

Keywords- Fracture, Wind turbine blade, J-Integral, FRP material, Stress Intensity Factor, Crack.

I. INTRODUCTION

Wind power technology has improved greatly in the last decade. The generating capacity of wind turbine has increased significantly, and the cost of generating power from wind has declined. Wind may be traced ultimately to the effect of the sun on the earth, including the lower portion of the atmosphere. The degradation of fossil fuel energy will induce the alternative renewable energy sources especially for wind energy.

The Horizontal axis wind turbines (HAWT) constitute the most common type of wind turbine in use today. In contrast to the mode of operation of the vertical axis wind turbines, the horizontal axis wind turbines need to be aligned with the direction of the wind, thereby allowing the wind to flow parallel to the axis of rotation. Insofar as concerns horizontal axis wind turbines, a distinction is made between upwind direction and downwind direction rotors.

The failure of the Horizontal axis wind turbine blades is the main cause of concern in the power generation. To identify the various causes of such failures a deep search in to the real time application of the wind turbine blades has been done. This study gave the clear idea about what different failures occur in the wind turbine blades and their consequences. A large number of works has been done in the area of wind turbine blade failures and their characteristics. A compilation of such work has been presented here.

The stress intensity factor was calculated by using j-integral method. The residual strength of brass at various crack lengths are studied [1].The static analysis of full 3-D finite element method and the critical zone where fatigue failure begins is extracted. A probabilistic model for analysis of the wind turbine rotor blade against failure. They consider only failure in flap wise during the normal operating condition of the wind turbine. The model is applied to an analysis of the reliability of the site-specific wind turbine of a prescribed make. The probability of the failure is in flap wise bending of the rotor blade is calculated by means of first-order reliability method [4]. A structural design for developing a medium scale composite wind turbine blade made of E-glass/epoxy for a 760 kW class horizontal axis wind turbine system. From the experimental results, it was found that the designed blade had structural integrity [5].

II. ROTOR BLADE MODELLING

A. Material

The Rotor blades are usually made up of a matrix of fiberglass mats, which are impregnated with a material such as polyester, thus the term glass fiber reinforced polyester. The polyester is hardened after it has impregnated the fiberglass. Epoxy is sometimes used instead of polyester.

Table:2.1. Rotor blade Material Properties

PROPERTIES	VALUES
Tensile Modulus Along X(Ex)	34000 M Pa
Tensile Modulus Along Y(Ey)	6530 M Pa
Tensile Modulus Along Z(Ez)	6530 M Pa
Shear Modulus along Xy(GXy)	2433 M Pa
Shear Modulus along Yz(GYz)	1698 M Pa
Shear Modulus along Zx(GZx)	2433 M Pa
Poisson Ratio along Xy(NU Xy)	0.217
Poisson Ratio along Yz(NU Yz)	0.366
Poisson Ratio along Zx(NU Zx)	0.217
Tensile Strength of Material	900 M Pa
Mass Density of Material (P)	2E-6 kg/ mm^3

B. Rotor blade dimensions

Table:2.2. Rotor blade dimensions

BLADE	DIMENSION
Blade Length	13000 mm
Max Root Chord	1651 mm
Tip Chord	647 mm
Blade Area	11.6 m^2
Twist	20.50 deg
Profile	NACA 4412
Blade Weight	900 Kg
Root Flange Outer Diameter	675 mm

C. Selection of airfoil

Selection of aerofoil is the important aspect of the blade modeling. Airplane wing and the turbine blades are selected in this manner. Here using NACA 4/5 software the selection of foil is carried out. Chosen of aerofoil is depends upon the Reynolds number of the flow over the aerofoil. Reynolds number of flow over the windmill blade is 196907.70127806097 according to this number company suggested the airfoil of the windmill blade is NACA 4412.Below figure represent the comparison of aerofoil in different digit family numbers, and the chosen aerofoil is also presented. Finalized airfoil for windmill blade is given below. This airfoil is used to model the blade. If you cross cut anywhere in the blade the cross section of the blade is Displayed like a below section. This airfoil having good lift and drag capacity that why this foil chooses in the windmill blade.

Fig:2.1. NACA 4412

D. Chord length determination

Eleven airfoil is made to build a blade each length of the chord very accurate one because this output is getting from the NACA package. The foil of maximum chord, and the minimum chord, and the intermediate chord all are the same that is in 4412.

Table:2.3. Airfoil chord length determination

FOIL	NO	CHORD (INCH)	CHORD (MM)
NACA 4412	1	65	1651
NACA 4412	2	61.05	1550.67
NACA 4412	3	57.1	1450.34
NACA 4412	4	53.15	1350.01
NACA 4412	5	49.2	1249.68
NACA 4412	6	45.25	1149.35
NACA 4412	7	41.3	1049.02
NACA 4412	8	37.35	948.69
NACA 4412	9	33.4	848.36
NACA 4412	10	29.45	748.03
NACA 4412	11	25.5	571.5

E. Twist setup

The blade is twisted along its axis to enable it to follow the change in the direction of the resulting wind along the blade, which the blade will experience when it rotates. Hence, the pitch will vary along the blade. The pitch is the angle between the chord of the blade profile and the rotor plane.

FOIL	NO	TWIST (DEG)
NACA 4412	1	0
NACA 4412	2	2.05
NACA 4412	3	4.1
NACA 4412	4	6.15
NACA 4412	5	8.2
NACA 4412	6	10.25
NACA 4412	7	12.3
NACA 4412	8	14.35
NACA 4412	9	16.4
NACA 4412	10	18.45
NACA 4412	11	20.50

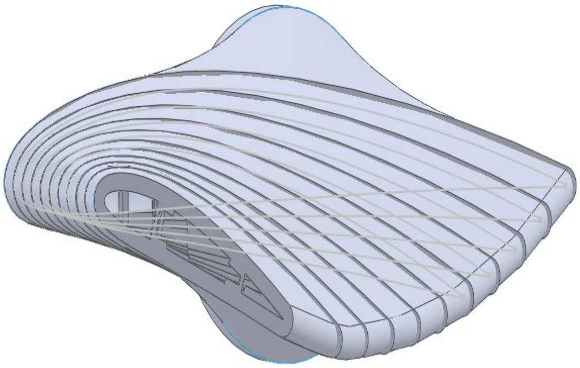

Fig :2.2 Twist setup of the blade (Front view)

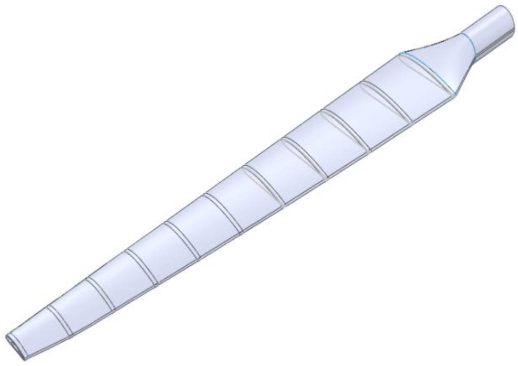

Fig :2.3 Final model of the HAWT rotor blade

Fig:2.4. Manufactured wind turbine blade and FRP material

Evaluation of Stress Intensity Factors

A finite element method provides a numerical method of stress intensity factor determination, which allows complex structure with general shape boundary and loading conditions to be readily handled. The finite element methods of determining the stress intensity factor are the displacement method or the stress method, energy methods such as strain energy release rate, **G line integrals (J-integral)** and a crack closure integral and the super position method. To alleviate the singularity problem with conventional finite element methods, several special crack tip finite elements have been developed which directly model the singularity at the crack tip. Here the ANSYS workbench is used for analyzing the semi elliptical crack of the Horizontal Axis Wind Turbine (HAWT) blade sample.

J-Integral :

To compute an energy quantity that describes the elastic-plastic behavior of materials, Rice introduced a contour integral that encloses the crack front shown in figure originally by Eshelby,

$$J = \int_{\Gamma} \left(W\,dy - T\frac{\partial \mu}{\partial x}\,ds \right)$$

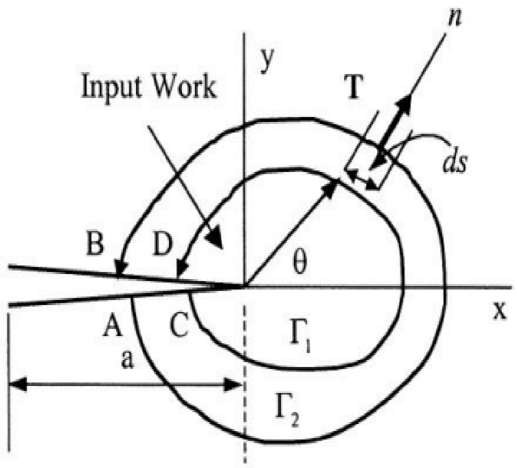

Fig:2.5 J-Integral contour around the crack surface

Where,

J = Effective energy release rate (M Pa.m or M N/m)

W = Elastic strain energy density or plastic loading work (j/m^3)

μ = Displacement vector at ds

ds = Differential Element of the contour

n = Outward unit normal to Γ

For anisotropic material,

$J=-1/2[K_I\ Im(m_{2i}\ N^{-1}_{ij}\ k_j)+K_{II}\ Im(m_{1i}\ N^{-1}_{ij}\ k_j)+K_{III}\ Im(m_{3i}\ N^{-1}_{ij}\ k_j)]$

$m_{1i}=S'_{11}-S'_{16}+S'_{12}+\lambda_i(S'_{15}\mu_i-S'_{14})$

$m_{2i}=S'_{21}-S'_{26}+S'_{22}/\mu_i+\lambda_i(S'_{25}-S'_{24}/\mu_i)$

$m_{3i}=S'_{41}-S'_{46}+S'_{42}/\mu_i+\lambda_i(S'_{45}-S'_{44}/\mu_i)$

$S'_{ij} = S_{ij}-[(S_{i3}*S_{3j})/S_{33}]$

Where, I,j=1,2,…,6

S'_{ij} = Material compliance tensor

μ_i = Eigen values of the compatibility equations with positive imaginary parts

$\lambda_i= -[l_3(\mu_i)/l_2(\mu_i)]$, i=1,2,3

$$N_{ij}=\begin{bmatrix} 1 & 1 & 1 \\ -\mu_1 & -\mu_2 & -\mu_3 \\ -\lambda_1 & -\lambda_2 & -\lambda_3 \end{bmatrix}$$

$N = N_{ij}$

N^{-1}_{ij}= Adjoint N_{ij} / Det (N)

III. ANSYS RESULTS

ANALYSIS-I

The major radius of the semielliptical crack is 10 mm and the minor radius is 6 mm and the applied pressure load is 100 N/mm^2.

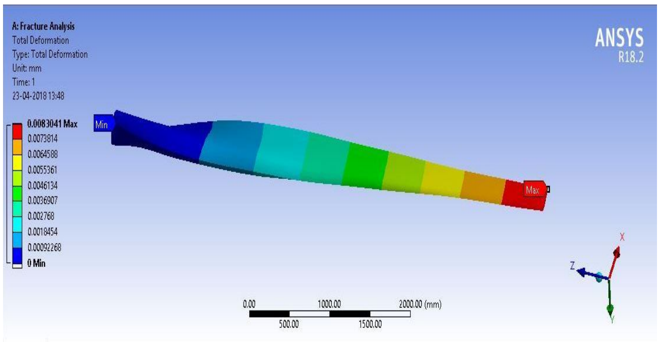

Fig: 3.1 Fracture analysis of HAWT blade

Model (A4) > Static Structural (A5) > Solution (A6) > Fracture Tool > SIFS (K1)

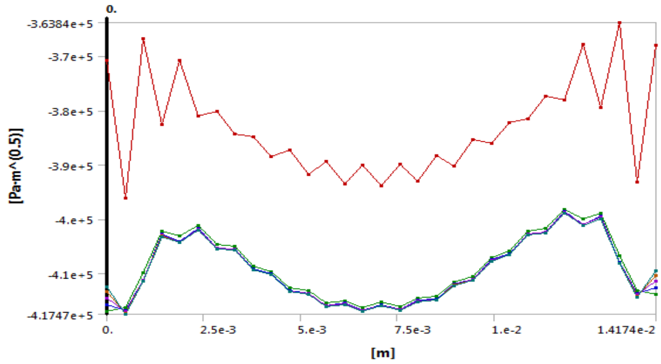

Graph:3.1.SIF(K1)

Model (A4) > Static Structural (A5) > Solution (A6) > Fracture Tool > SIFS (K1)

Length [m]	SIFS (K1) Contour 1 [Pa·m^(0.5)]	SIFS (K1) Contour 2 [Pa·m^(0.5)]	SIFS (K1) Contour 3 [Pa·m^(0.5)]	SIFS (K1) Contour 4 [Pa·m^(0.5)]	SIFS (K1) Contour 5 [Pa·m^(0.5)]	SIFS (K1) Contour 6 [Pa·m^(0.5)]
0.	-3.708e+005	-4.1689e+005	-4.158e+005	-4.1445e+005	-4.1339e+005	-4.1248e+005
4.723e-004	-3.9615e+005	-4.1626e+005	-4.1676e+005	-4.1703e+005	-4.173e+005	-4.1747e+005
9.4455e-004	-3.6672e+005	-4.0991e+005	-4.1115e+005	-4.1131e+005	-4.1141e+005	-4.1146e+005
1.4169e-003	-3.8259e+005	-4.022e+005	-4.0269e+005	-4.0291e+005	-4.0311e+005	-4.032e+005
1.8892e-	-3.7084e	-4.0315e	-4.0418e	-4.0429e	-4.0435e	-4.0435e

003	+005	+005	+005	+005	+005	+005
2.3617e-003	-3.8105e+005	-4.0124e+005	-4.0169e+005	-4.0183e+005	-4.0195e+005	-4.0196e+005
2.8341e-003	-3.8011e+005	-4.0455e+005	-4.0529e+005	-4.054e+005	-4.0546e+005	-4.0548e+005
3.3066e-003	-3.8425e+005	-4.05e+005	-4.0545e+005	-4.0557e+005	-4.0568e+005	-4.057e+005
3.7791e-003	-3.8486e+005	-4.0857e+005	-4.0917e+005	-4.0927e+005	-4.0935e+005	-4.0937e+005
4.2516e-003	-3.8845e+005	-4.0958e+005	-4.1002e+005	-4.1015e+005	-4.1024e+005	-4.1026e+005
4.7241e-003	-3.8734e+005	-4.1261e+005	-4.1314e+005	-4.1325e+005	-4.1333e+005	-4.1336e+005
5.1967e-003	-3.9179e+005	-4.1317e+005	-4.1362e+005	-4.1374e+005	-4.1383e+005	-4.1385e+005
5.6693e-003	-3.8935e+005	-4.1532e+005	-4.1583e+005	-4.1594e+005	-4.1602e+005	-4.1605e+005
6.1418e-003	-3.9353e+005	-4.1502e+005	-4.1547e+005	-4.1559e+005	-4.1568e+005	-4.157e+005
6.6144e-003	-3.9006e+005	-4.1624e+005	-4.1674e+005	-4.1685e+005	-4.1694e+005	-4.1698e+005
7.087e-003	-3.9379e+005	-4.1529e+005	-4.1575e+005	-4.1587e+005	-4.1597e+005	-4.16e+005
7.5596e-003	-3.8987e+005	-4.1604e+005	-4.1653e+005	-4.1665e+005	-4.1673e+005	-4.1677e+005
8.0321e-003	-3.9302e+005	-4.1447e+005	-4.1492e+005	-4.1504e+005	-4.1514e+005	-4.1515e+005
8.5047e-003	-3.883e+005	-4.1421e+005	-4.1471e+005	-4.1482e+005	-4.1491e+005	-4.1493e+005
8.9773e-003	-3.9023e+005	-4.1152e+005	-4.1196e+005	-4.1208e+005	-4.1218e+005	-4.1219e+005
9.4499e-003	-3.8534e+005	-4.1047e+005	-4.11e+005	-4.1111e+005	-4.1119e+005	-4.1121e+005
9.9224e-003	-3.8604e+005	-4.0704e+005	-4.0748e+005	-4.0761e+005	-4.077e+005	-4.0772e+005
1.0395e-002	-3.8229e+005	-4.0583e+005	-4.0642e+005	-4.0653e+005	-4.066e+005	-4.0662e+005
1.0867e-002	-3.816e+005	-4.022e+005	-4.0264e+005	-4.0277e+005	-4.0286e+005	-4.0287e+005
1.134e-002	-3.7737e+005	-4.0159e+005	-4.0234e+005	-4.0244e+005	-4.025e+005	-4.025e+005
1.1812e-002	-3.7815e+005	-3.9817e+005	-3.9861e+005	-3.9876e+005	-3.9888e+005	-3.989e+005
1.2285e-002	-3.6789e+005	-3.9993e+005	-4.0095e+005	-4.0106e+005	-4.0113e+005	-4.0113e+005
1.2757e-002	-3.7953e+005	-3.9897e+005	-3.9946e+005	-3.9967e+005	-3.9987e+005	-3.9995e+005
1.3229e-002	-3.6384e+005	-4.0666e+005	-4.0789e+005	-4.0805e+005	-4.0815e+005	-4.0818e+005
1.3702e-002	-3.9318e+005	-4.1312e+005	-4.1361e+005	-4.1388e+005	-4.1416e+005	-4.1434e+005
1.4174e-002	-3.6804e+005	-4.1376e+005	-4.1269e+005	-4.1137e+005	-4.1034e+005	-4.0953e+005

Table:3.1. SIF(K1)

Model (A4) > Static Structural (A5) > Solution (A6) > Fracture Tool > SIFS (K2)

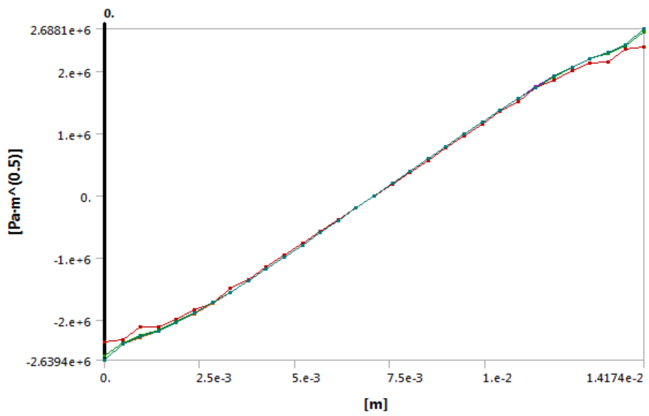

Graph:3.2.SIF(K2)

Model (A4) > Static Structural (A5) > Solution (A6) > Fracture Tool > SIFS (K2)

Length [m]	SIFS (K2) Contour 1 [Pa·m^(0.5)]	SIFS (K2) Contour 2 [Pa·m^(0.5)]	SIFS (K2) Contour 3 [Pa·m^(0.5)]	SIFS (K2) Contour 4 [Pa·m^(0.5)]	SIFS (K2) Contour 5 [Pa·m^(0.5)]	SIFS (K2) Contour 6 [Pa·m^(0.5)]
0.	-2.3448e+006	-2.5789e+006	-2.6325e+006	-2.6387e+006	-2.6394e+006	-2.6374e+006
4.723e-004	-2.313e+006	-2.3713e+006	-2.3763e+006	-2.3785e+006	-2.3805e+006	-2.382e+006
9.4455e-004	-2.1082e+006	-2.2428e+006	-2.2734e+006	-2.2722e+006	-2.2697e+006	-2.2669e+006
1.4169e-003	-2.1033e+006	-2.1628e+006	-2.1656e+006	-2.1666e+006	-2.1677e+006	-2.1683e+006
1.8892e-003	-1.981e+006	-2.021e+006	-2.038e+006	-2.0361e+006	-2.0337e+006	-2.0312e+006
2.3617e-003	-1.8233e+006	-1.8872e+006	-1.889e+006	-1.8893e+006	-1.8894e+006	-1.8892e+006
2.8341e-003	-1.7175e+006	-1.716e+006	-1.7224e+006	-1.7205e+006	-1.7185e+006	-1.7164e+006
3.3066e-003	-1.4925e+006	-1.5491e+006	-1.5502e+006	-1.5499e+006	-1.5495e+006	-1.549e+006
3.7791e-003	-1.3409e+006	-1.3636e+006	-1.3656e+006	-1.3641e+006	-1.3625e+006	-1.3609e+006
4.2516e-003	-1.1337e+006	-1.178e+006	-1.1786e+006	-1.1782e+006	-1.1777e+006	-1.177e+006
4.7241e-003	-9.5055e+005	-9.8547e+005	-9.8608e+005	-9.8498e+005	-9.8388e+005	-9.8272e+005
5.1967e-003	-7.6116e+005	-7.9108e+005	-7.9139e+005	-7.9102e+005	-7.9061e+005	-7.9012e+005
5.6693e-003	-5.6991e+005	-5.9487e+005	-5.9505e+005	-5.9439e+005	-5.9374e+005	-5.9304e+005
6.1418e-003	-3.8231e+005	-3.9734e+005	-3.9747e+005	-3.9726e+005	-3.9704e+005	-3.9676e+005
6.6144e-003	-1.9041e+005	-1.991e+005	-1.9913e+005	-1.9891e+005	-1.9869e+005	-1.9845e+005
7.087e-003	-232.89	-141.48	-134.79	-128.19	-122.66	-118.39
7.5596e-003	1.9039e+005	1.994e+005	1.9945e+005	1.9924e+005	1.9904e+005	1.9882e+005
8.0321e-003	3.8371e+005	3.9902e+005	3.9917e+005	3.9898e+005	3.9877e+005	3.9851e+005
8.5047e-003	5.7334e+005	5.9896e+005	5.9915e+005	5.9851e+005	5.9788e+005	5.9721e+005
8.9773e-003	7.676e+005	7.981e+005	7.9844e+005	7.9808e+005	7.9768e+005	7.972e+005
9.4499e-003	9.5986e+005	9.961e+005	9.9673e+005	9.9565e+005	9.9458e+005	9.9344e+005
9.9224e-003	1.1473e+006	1.1926e+006	1.1932e+006	1.1928e+006	1.1923e+006	1.1917e+006
1.0395e-002	1.3576e+006	1.383e+006	1.385e+006	1.3835e+006	1.382e+006	1.3804e+006
1.0867e-002	1.5151e+006	1.5734e+006	1.5744e+006	1.5741e+006	1.5738e+006	1.5732e+006
1.134e-002	1.7423e+006	1.7453e+006	1.7516e+006	1.7497e+006	1.7478e+006	1.7457e+006
1.1812e-002	1.8546e+006	1.9207e+006	1.9226e+006	1.9228e+006	1.9229e+006	1.9227e+006
1.2285e-002	2.0133e+006	2.0591e+006	2.0758e+006	2.074e+006	2.0716e+006	2.0692e+006
1.2757e-002	2.1414e+006	2.2039e+006	2.2067e+006	2.2077e+006	2.2088e+006	2.2094e+006
1.3229e-002	2.1463e+006	2.2871e+006	2.3173e+006	2.3161e+006	2.3136e+006	2.3109e+006
1.3702e-002	2.3547e+006	2.4165e+006	2.4214e+006	2.4237e+006	2.4257e+006	2.4272e+006

1.4174e-002	2.3868e+006	2.628e+006	2.6813e+006	2.6875e+006	2.6881e+006	2.6859e+006

Table:3.2. SIF(K2)

Model (A4) > Static Structural (A5) > Solution (A6) > Fracture Tool > SIFS (K3)

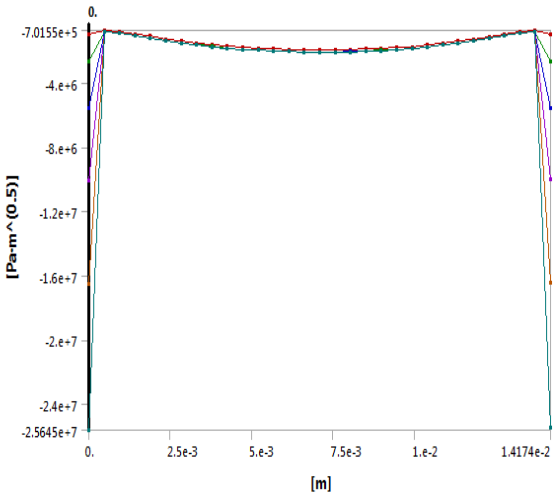

Graph:3.3. SIF(K3)

Model (A4) > Static Structural (A5) > Solution (A6) > Fracture Tool > SIFS (K3)

Length [m]	SIFS (K3) Contour 1 [Pa·m^(0.5)]	SIFS (K3) Contour 2 [Pa·m^(0.5)]	SIFS (K3) Contour 3 [Pa·m^(0.5)]	SIFS (K3) Contour 4 [Pa·m^(0.5)]	SIFS (K3) Contour 5 [Pa·m^(0.5)]	SIFS (K3) Contour 6 [Pa·m^(0.5)]
0.	-9.1844e+005	2.6458e+006	5.5626e+006	1.0029e+007	1.6512e+007	2.5645e+007
4.723e-004	-7.0155e+005	-7.5421e+005	-7.5494e+005	-7.5565e+005	-7.5636e+005	-7.5703e+005
9.4455e-004	-7.6478e+005	-8.6253e+005	-8.6382e+005	-8.6476e+005	-8.6539e+005	-8.6581e+005
1.4169e-003	-9.4231e+005	-1.0011e+006	-1.0033e+006	-1.0047e+006	-1.0054e+006	-1.0058e+006
1.8892e-003	-1.0602e+006	-1.1728e+006	-1.1741e+006	-1.1746e+006	-1.1751e+006	-1.1754e+006
2.3617e-003	-1.2452e+006	-1.3181e+006	-1.3194e+006	-1.3199e+006	-1.3203e+006	-1.3206e+006
2.8341e-003	-1.3546e+006	-1.4752e+006	-1.4767e+006	-1.4772e+006	-1.4777e+006	-1.478e+006
3.3066e-003	-1.5016e+006	-1.5893e+006	-1.591e+006	-1.5916e+006	-1.5921e+006	-1.5925e+006
3.7791e-003	-1.5857e+006	-1.7094e+006	-1.711e+006	-1.7116e+006	-1.7121e+006	-1.7125e+006
4.2516e-003	-1.6973e+006	-1.796e+006	-1.7977e+006	-1.7983e+006	-1.7988e+006	-1.7992e+006
4.7241e-003	-1.7515e+006	-1.883e+006	-1.8847e+006	-1.8854e+006	-1.8859e+006	-1.8863e+006
5.1967e-003	-1.8326e+006	-1.939e+006	-1.9409e+006	-1.9415e+006	-1.9421e+006	-1.9425e+006
5.6693e-003	-1.859e+006	-1.9961e+006	-1.998e+006	-1.9987e+006	-1.9992e+006	-1.9997e+006
6.1418e-003	-1.9129e+006	-2.0239e+006	-2.0258e+006	-2.0264e+006	-2.027e+006	-2.0275e+006
6.6144e-003	-1.9134e+006	-2.0533e+006	-2.0552e+006	-2.0559e+006	-2.0565e+006	-2.0569e+006
7.087e-003	-1.9416e+006	-2.0542e+006	-2.0561e+006	-2.0568e+006	-2.0574e+006	-2.0579e+006
7.5596e-003	-1.9168e+006	-2.057e+006	-2.0589e+006	-2.0597e+006	-2.0602e+006	-2.0607e+006
8.0321e-003	-1.9197e+006	-2.0311e+006	-2.033e+006	-2.0337e+006	-2.0343e+006	-2.0348e+006
8.5047e-003	-1.8688e+006	-2.0067e+006	-2.0086e+006	-2.0093e+006	-2.0098e+006	-2.0102e+006
8.9773e-003	-1.8452e+006	-1.9524e+006	-1.9542e+006	-1.9549e+006	-1.9554e+006	-1.9559e+006
9.4499e-003	-1.7662e+006	-1.8987e+006	-1.9005e+006	-1.9012e+006	-1.9017e+006	-1.9021e+006
9.9224e-003	-1.7137e+006	-1.8134e+006	-1.8152e+006	-1.8158e+006	-1.8163e+006	-1.8167e+006

1.0395e-002	-1.6031e+006	-1.7281e+006	-1.7298e+006	-1.7304e+006	-1.7309e+006	-1.7313e+006
1.0867e-002	-1.5195e+006	-1.6083e+006	-1.61e+006	-1.6106e+006	-1.6111e+006	-1.6115e+006
1.134e-002	-1.3717e+006	-1.4938e+006	-1.4953e+006	-1.4958e+006	-1.4963e+006	-1.4966e+006
1.1812e-002	-1.2614e+006	-1.3352e+006	-1.3366e+006	-1.3371e+006	-1.3375e+006	-1.3378e+006
1.2285e-002	-1.0742e+006	-1.1883e+006	-1.1896e+006	-1.1902e+006	-1.1906e+006	-1.1909e+006
1.2757e-002	-9.5454e+005	-1.0142e+006	-1.0164e+006	-1.0178e+006	-1.0185e+006	-1.0189e+006
1.3229e-002	-7.7459e+005	-8.7374e+005	-8.7504e+005	-8.76e+005	-8.7663e+005	-8.7707e+005
1.3702e-002	-7.1058e+005	-7.6397e+005	-7.647e+005	-7.6542e+005	-7.6613e+005	-7.6681e+005
1.4174e-002	-9.2244e+005	-2.6398e+006	-5.537e+006	-9.9712e+006	-1.6406e+007	-2.5466e+007

Table:3.3. SIF (K3)

Model (A4) > Static Structural (A5) > Solution (A6) > Fracture Tool > J-Integral (JINT)

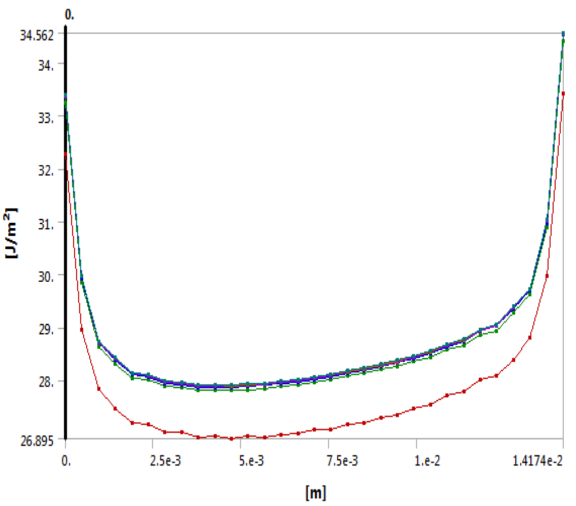

Graph:3.4. J-integral

Model (A4) > Static Structural (A5) > Solution (A6) > Fracture Tool > J-Integral (JINT)

Length [m]	J-Integral (JINT) Contour 1 [J/m²]	J-Integral (JINT) Contour 2 [J/m²]	J-Integral (JINT) Contour 3 [J/m²]	J-Integral (JINT) Contour 4 [J/m²]	J-Integral (JINT) Contour 5 [J/m²]	J-Integral (JINT) Contour 6 [J/m²]
0.	32.283	33.249	33.367	33.379	33.392	33.397
4.723e-004	28.954	29.836	29.914	29.96	29.982	29.982
9.4455e-004	27.829	28.62	28.701	28.719	28.729	28.732
1.4169e-003	27.463	28.313	28.389	28.406	28.429	28.44
1.8892e-003	27.197	28.037	28.111	28.125	28.136	28.142
2.3617e-003	27.174	28.001	28.065	28.084	28.102	28.112
2.8341e-003	27.018	27.878	27.949	27.966	27.98	27.988
3.3066e-003	27.008	27.855	27.92	27.941	27.959	27.97
3.7791e-003	26.918	27.803	27.869	27.887	27.902	27.912
4.2516e-003	26.943	27.812	27.872	27.893	27.909	27.921
4.7241e-003	26.895	27.801	27.863	27.882	27.897	27.909
5.1967e-003	26.938	27.825	27.883	27.904	27.92	27.933
5.6693e-003	26.92	27.842	27.901	27.92	27.937	27.949
6.1418e-003	26.981	27.882	27.938	27.959	27.975	27.989
6.6144e-003	26.984	27.915	27.972	27.992	28.009	28.022
7.087e-003	27.059	27.967	28.022	28.043	28.059	28.073
7.5596e-003	27.077	28.012	28.069	28.089	28.106	28.119
8.0321e-003	27.167	28.074	28.131	28.152	28.168	28.181
8.5047e-003	27.195	28.126	28.185	28.205	28.222	28.234
8.9773e-003	27.301	28.2	28.259	28.28	28.296	28.309

9.4499e-003	27.341	28.262	28.325	28.344	28.36	28.372
9.9224e-003	27.474	28.359	28.42	28.442	28.458	28.47
1.0395e-002	27.53	28.435	28.502	28.521	28.536	28.546
1.0867e-002	27.703	28.572	28.637	28.658	28.676	28.687
1.134e-002	27.779	28.663	28.736	28.754	28.768	28.777
1.1812e-002	28.001	28.854	28.918	28.937	28.955	28.964
1.2285e-002	28.074	28.942	29.018	29.032	29.044	29.05
1.2757e-002	28.396	29.275	29.353	29.369	29.391	29.401
1.3229e-002	28.8	29.619	29.703	29.722	29.732	29.736
1.3702e-002	29.977	30.889	30.97	31.017	31.039	31.036
1.4174e-002	33.409	34.408	34.53	34.543	34.557	34.562

Table:3.4. J-integral

Similarly, for different load conditions such as 150 N/mm^2, 200 N/mm^2, 250 N/mm^2 the Stress Intensity Factors and J- Integral values are calculated.

IV. CONCLUTION

In this work the selection of Airfoil NACA 4421 and their design calculations has been calculated. The blade model was designed in Solid works and this model was Fracture Analyzed in ANSYS Workbench. The numerical values of Stress Intensity Factors and J-Integral values has been calculated for different load conditions, such as, 100 N/mm^2, 150 N/mm^2, 200 N/mm^2 and 250 N/mm^2.The scaled model of wind turbine blade was manufactured by using hand lay method. The material used for manufacture of this scaled model is Glass Fiber Reinforced Polyester.

V. FUTURE WORK

In future the manufactured scaled model of wind turbine blade will be fatigue analyzed experimentally then the experimental values and the simulated numerical values will be compared and the percentage error will be calculated. Also, finally the life of wind turbine blade will be predicted.

REFERENCES

[1] Jui-sheng chou, Wan-Ting Tu, September 2010, “Failure analysis and risk management of a collapsed large wind turbine tower “, ELSEVIER, Vol. No.18, pages: 295-313.

[2] C.Kong, J.Bang, Y.Sugiyama, August 2005, “Structural investigation of composite wind turbine blade considering various load cases and fatigue life”, ELSEVIER, Vol.No.30, Pages:2101-2114

[3] Knut O. Ronold, Gunner C. Larsen, September 2000, “Reliability based design of wind-turbine rotor blades against failure in ultimate loading”, Vol.No. 22, Pages: 565- 574.

[4] P.J.Tavner, J.Xiang, F.Spinato,et.,al., July 2007, “Reliability analysis for wind turbines”,John wiley, Vol.No.10, Pages:1-18

[5] Paul S.Veers, Thomas D.Ashwill,et.,al., December 2003,” Trends in the design, Manufacture and Evaluation of Wind Turbine Blades”, John Wiley, Vol.No.6, Pages:245-259

[6] Fausto Pedro Garcia Marquez, Andrew Mark Tobias,et.al.,” Renewable Energy “ ELSEVIER, Vol.No.46, Pages: 169-178.

[7] Yssine Amirat, Mohamed Benbouzid,et.al., October 2010,”A brief status on condition monitoring and fault diagnosis in wind energy conversion system”,ELSEVIER, Vol.No.3(9), Page No: 2629-2636.

[8] Mahmood M.Shokrieh, Roham Rafiee, June 2006, “Simulation of fatigue failure in a full composite wind turbine blade”, ELSEVIER, Vol.No.74, Page No:332-342.

[9] YaoHsu, Wen-FangWu, Yung-Chang Chang, December 2014, “Reliability Analysis of Wind Turbine Towers”, ELSEVIER, Vol.No.79, Page NO: 218-224.67

[10] Chia Chen Ciang. Structural health monitoring for a wind turbine system:a review of damage detection methods. IOP publishing, pages 1-20, 2008.

[11] M. A. Eder, R. D. Bitsc,April 2014,” Fracture analysis of adhesive joints in wind turbine blades”, Whiley Publication, Vol.No.18, Page No:1007-1022.